Laser Dicing of Silicon: Comparison of Ablation Mechanisms with a Novel Technology of Thermally Induced Stress

Oliver HAUPT, Frank SIEGEL, Aart SCHOONDERBEEK, Lars RICHTER, Rainer KLING, Andreas OSTENDORF

Laser Zentrum Hannover e.V. Hollerithallee 8, D-30419 Hannover, Germany
E-mail: o.haupt@lzh.de

The major issue for dicing of silicon is the edge quality with corresponding die strength. We compared the influence of pulse duration and cutting speed with the corresponding edge quality by using a three-point bending test. As a result the bending strength of the cut samples directly correlates with edge defects. In contrast to the laser dicing technologies using ablation, we investigated a novel mechanism of thermally induced stress cutting of silicon wafers. This process does not produce any debris or other edge defects and uses continuous wave laser radiation. One-step cutting for wafers is possible up to a thickness of a several hundred microns if laser radiation with photon energy near the indirect band gap of silicon is used. The results of ablation rates and bending strength will be presented from picosecond to continuous wave laser dicing.

Keywords: silicon, laser, cutting, bending strength, thermally induced stress

1. Introduction

The fragility of silicon is one of the main issues when talking about processing, e.g. cutting or scribing due to the tendency of thinner wafers. Separating of silicon becomes more important in micro-technology and photovoltaic applications. Therefore, non-contact processes like laser cutting by ablation techniques can be used and investigations have been done to improve the edge quality [1,2,4,5]. Further, a stealth dicing technology is known, where a layer inside of the material is modified by using a semi-transparent laser wavelength and positioning the laser spot inside the material [3]. The main challenge of processing silicon with laser radiation is to avoid or reduce damage and debris. Laser ablation is a process where a part of the silicon will be melted or sublimated inside the material interaction zone. As the interaction time between the laser radiation and the lattice is lengthened, more heat is conducted into the bulk silicon [6]. The effect of ablation is dependent on laser power and pulse duration. These parameters also directly affect the quality of a cut and the die strength, but further research is needed to investigate the relationship.

The fracture strength of cut silicon wafers with different laser sources, their corresponding pulse durations and wavelengths, have to be investigated in detail. Furthermore, a new cutting process using thermally controlled cracking will be investigated and compared with different ablation processes using the bending strength approach as the relevant parameter.

The ablation behavior of different laser sources with corresponding pulse duration and wavelengths are investigated in the beginning to find process parameters for successfully cutting of the silicon samples. This is the basis to show the strength of crystal silicon samples across different dicing processes.

2. Properties of silicon

To process silicon two main parameters are accounted for: The optical penetration depth d_α and the thermal diffusion length l_d which is also strongly connected to the pulse duration τ_P of the used laser system. The optical penetration depth is the reciprocal of the absorption coefficient α which is strongly dependent on the wavelength of the laser source and the temperature of the silicon [7]. The absorption coefficient increases with increasing temperatures and leads to decreasing optical penetration depths within the laser interaction time. A significant transition of the optical properties can be observed at the indirect band-gap of silicon at $E_g = 1.12\ eV$ or $\lambda = 1.107\ \mu m$ at room temperature. In Figure 1 the optical and heat diffusion length are shown.

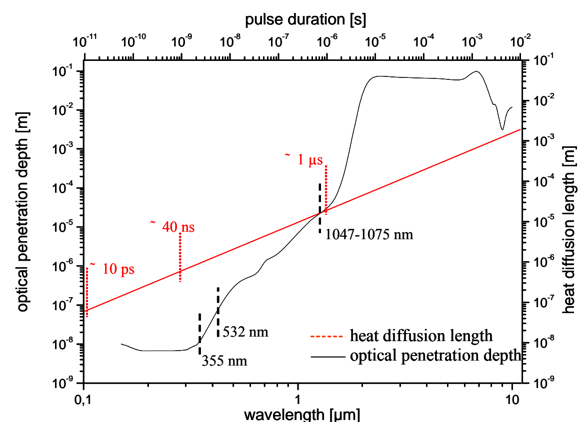

Fig. 1 Dependence of heat diffusion length over pulse duration and optical penetration length over wavelength [8,9].

It can be shown that for wavelengths near the indirect band-gap the depth of the optical penetration has the same dimensions like the investigated wafer thickness of

s ≈ 220 µm. Shorter wavelengths lead to lower optical penetration depth. With λ = 355 nm d_α is reduced to approx. 10 nm. The second parameter, the heat diffusion length, increases with increasing pulse duration. Typically pulse durations are micro-, nano- and picoseconds with heat diffusions length of $l_d = 900 / 1 / 0.1$ µm. As shown for pulse durations below micro-seconds the heat diffusion length is higher than the optical penetration depth.

The consideration of the optical and thermal behavior during laser ablation with different pulse durations and wavelengths leads to an assumption that longer pulse durations leads to higher ablation ratio as well as longer wavelengths as investigated partially [10,11]

3. Experimental work

To determine the effects of various cutting speeds with different laser processes on the quality of a cut, three main investigations are done. First, the respective ablation ratio for defined pulse durations and wavelengths are determined. In the second part, cutting of silicon by thermally induced stress is investigated. In the last part the characteristic strength of the cut samples is measured in detail.

3.1 Cutting by laser ablation

Before the test samples for the bending tests are cut the ablation ratio has to be determined. Firstly an array of ablation lines configured with different parameters is performed on a s =500 µm thick silicon wafer. The number of cycles are set to n = 1-5-10 and the cutting speeds are set from V_f = 10 mm/s up to 1000 mm/s. This array is processed over the full range of possible output powers for each corresponding laser source. The depth of each ablated groove is then measured and by using the Equation 1, the ablation ratio per pulse a_P can be calculated.

$$a_P = \left(\frac{a_d}{\frac{d_F * f_P}{V_f}} \right) \quad (1)$$

a_d is the total measured depth of the groove, d_F is the focus diameter (1/e²), f_P is the frequency of repetitions of the laser and V_f is the feed rate of the scanner. The basis for comparison of different laser sources and pulse duration is the energy in dependence of the pulse duration, the fluence H_P. Laser sources with pulse durations τ_P ranging from pico-seconds up to micro-seconds are used with corresponding parameters as listed in Table 1. Scanners are used to guide the laser beams.

Table 1 Laser sources used for dicing by ablation.

Laser	Wave-length λ [nm]	Pulse duration τ_P	Focal length [mm]	Focus size [µm]
a Rofin StarDisc	1030	≈ 1µs	163	≈ 16
b Lumera Staccato	1064	≈ 12ps	100	≈ 28
c Trumpf TL20-FQ	1047	≈ 50ns	100	≈ 35
d Coherent Avia7	355	≈ 20ns	160	≈ 28
e Coherent Avia20	355	≈ 40ns	160	≈ 28

The two Avia laser from Coherent are used to investigate the influence of pulse duration and repetition rate.

3.2 Cutting by thermally induced stress

Cutting by thermally induced stress does not involve any ablation or structural changes to the lattice. In the range of semi transparency of crystal silicon near the indirect band-gap, a phonon assisted absorption process occurs and heats up the material to a defined temperature [9]. This temperature rise leads to a defined stress profile around the laser spot and due to relative movement, a distortion is generated and can be expressed by Equation 2.

$$E_{\varepsilon i} = \sum {}_j T_{ij} \sigma_j \quad (2)$$

Here, tensor T_{ij} contains the Poisson´s ratio and give a relation between tensile and compression stress. The σ_j is the generated stress and depends on the direction where the heat spot moves.

Due to the wavelength of the used laser source near the indirect band-gap the model of volume heating is relevant and will be taken to explain the cutting mechanism. If the material is heated a thermal expansion of the interaction zone can be observed. The expansion again leads to a defined stress profile in and around the laser spot and generates a stress difference between tensile and compressive stress. If the generated stress crosses the critical stress of crystalline silicon a crack is produced and can be guided along the heating path of the laser. The phenomena is used to cut silicon samples out of a wafer with <111> and <100> orientation and a thicknesses of s = 220 µm. The cutting speed varies from V_f =8 mm/s to 50 mm/s by using axis with linear movement. The limitation of the cutting speed is here due to the maximum available speed of the precision axis system. For the comparison with the ablation technologies the used speed is comparable to the effective cutting speed of ablation technologies due to the necessary repetitions to cut through the wafer. The laser source used is a continuous wave fiber-laser with parameters shown in Table 2.

Table 2 Laser source used for dicing by thermally induced stress.

Laser	Wave-length λ [nm]	Pulse duration τ_P	Focal length [mm]	Focus size [µm]
SPI Fiber Laser	1075	cw	80	≈40

The main focus of this paper is to compare the mechanical strength of silicon samples produced with industrial available laser sources and a new process as explained briefly. The results e.g. process borders and a detailed description of the process of thermally induced stress (LIS) will be presented in a separate paper which will published in the future.

3.3 Characteristic bending strength

For the evaluation of the edge quality a three point bending test is used as shown in Figure 2. With this set-up the force to break the respective sample can be measured and is the basis for the fracture characterization. Statistical methods are applied to derive reliable material parameters from the investigations. The Weibull theory is the common method for brittle materials [12]. The probability of failure

(Received: June 16, 2008, Accepted: October 1, 2008)

P_f of specimens which are subjected to a certain stress can be calculated with Equation 3.

$$P_f = 1 - \exp\left(-\frac{\sigma}{\sigma_\theta}\right)^m \quad (3)$$

σ_θ is the characteristic strength, σ is the applied stress and m is the Weibull-modulus, which describes the scattering. The characteristic strength is where 63.2 % of the samples fail.

bending tester:	XYZTEC Condor 70	distance a:	9 mm
max. force:	80 N	sample width w:	3 mm
bending velocity: 50 µm/s		sample thickness d: varies	

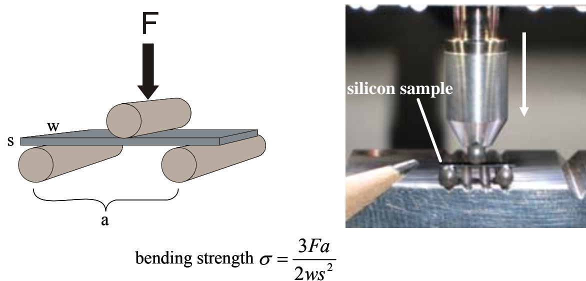

Fig. 2 Bending test set-up to determine the characteristic bending strength.

The characteristic bending strength directly correlates with mechanical damages found on the cut [13]. To compare the edge quality produced with different pulse durations and power, all samples have the same size of 12 mm by 3 mm (l x w).

4. Results

The ablation depths per pulse for different pulse durations and wavelengths are the basis for determining the number of cycles which are necessary to separate the material over its whole thickness. Thus, the wafer is cut so that the ablated array can be measured with a microscope. In Figure 3 the ablation depths per pulse a_P is shown in dependence of the fluence H_P

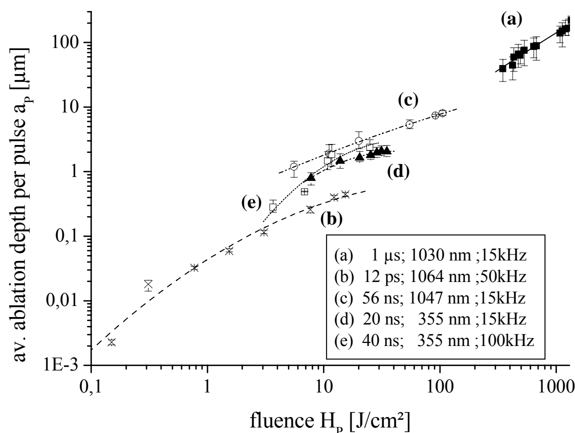

Fig. 3 Average ablation depth per pulse a_P in dependence of the fluence H_P for different laser sources.

It can be clearly shown that the average ablation depth per pulse is below 1 µm for the picosecond-system while for the µs-system an average depth of around 100 µm can be observed but the fluence here is more than 100 times higher than for the picosecond laser. In the range where a comparable fluence can be found for different wavelengths and pulse durations no significant differences occur. The comparison of (c, d and e) with wavelengths of λ = 1047 nm and 355 nm and pulse durations from τ_P = 20 to 56 ns shows an average ablation ratio per pulse of $a_P \approx$ 1-2 µm at fluences of $H_P \approx$ 10 J/cm^2.

To reach an acceptable edge quality, a pulse overlap O_P of 50 % to 60 % is implemented. The actual ablation depth a_d in dependence of the fluence can be shown in Figure 4 for a pulse overlap between 52 % and 64 %. Here the real ablation depth is shown for the listed cutting speed V_f with a corresponding repetition rate of the laser source.

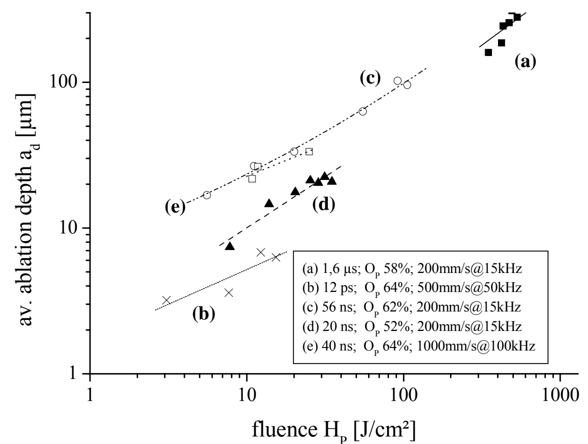

Fig. 4 Average ablation depth a_d in dependence of the fluence H_P and pulse overlap O_P at 5 cycles, (a) with 4 cycles.

Again, the comparison of (c and e) with same pulse overlaps but different wavelengths shows that there are no significant differences in total ablation ratio. In contrast to that the picosecond laser produces an approx. 10 times lower ablation depth using the same fluence. With defined overlaps, maximum repetition rates, and cutting speed the minimum necessary number of cycles for each laser system is investigated.

The wafer thickness for the investigations is s = 220 µm. In order to cut different samples of the same size, the number of cycles n to cut the samples is dependent on the pulse energy E_P that is defined in Table 3. The number of cycles and the scanning rate V_f leads to an effective cutting speed V_{fe} for the corresponding wafer thickness by calculating $V_{fe} = V_f$ / n. A safety factor of 10% for number of cycles necessary to cut through is included within the listed number of cycles.

The results are based on the comparison of the fluence where the deviations of the spot diameter are eliminated. A look at the difference in cutting speeds and pulse energy of the corresponding laser sources shows a principle effect of scaling the effective cutting speed with the pulse energy. Here an approx. 10 times higher pulse energy leads to a 10 times higher effective cutting speed if a) and d) or e) are

compared even though the wavelengths and therefore the optical penetration depths are differing by a factor of 3.

Table 3 Samples cut with number of cycles n and pulse energy E_P.

Laser	No. of cycles n	Pulse energy E_P	Scanning rate V_F	Effective cutting speed V_{Fe}
a StarDisc	6	1760 µJ	200mm/s	33,3mm/s
b Staccato	500	96 µJ	300mm/s	0.6mm/s
c TLQ20	25	700 µJ	200mm/s	8mm/s
d Avia7	200	141 µJ	300mm/s	1.5mm/s
e Avia20	200	150 µJ	600mm/s	3mm/s

Additionally the cutting speed of b) with the lowest pulse energy is slow. Here a number of $n = 500$ cycles is necessary to cut a wafer of $s = 220$ µm and therefore is not suitable for dicing with a view to industrial requirements. For all listed cutting speeds the delay times are neglected. All samples are cut with the same layout.

4.1 Cutting by thermally induced stress (LIS)

As explained in Section 3.2 the process of thermally induced stress is used to produce samples of the same size than for ablation technologies. To use the separation process, the lower limit of power density is defined and is used to separate the crystalline silicon along a defined path. The parameter and a typical SEM picture of a produced crack is shown in Figure 5. The main parameter is the power density I_0. The variables are power, focus diameter, and velocity. The listed parameter leads to a damage free surface. The laser spot is $z = 5$ mm above the silicon surface which leads to focus diameter on the surface of $d_f = 443$ µm. The irradiated laser power is $P_{AV} = 25.8$ Watts.

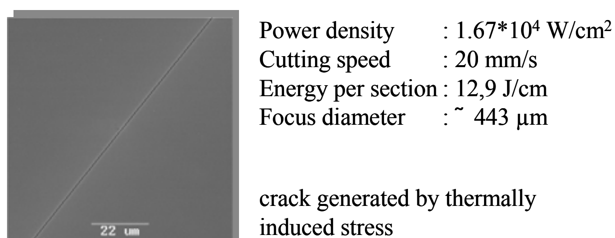

Fig. 5 SEM image of cut silicon sample without surface damages.

These parameters are used to cut the number of samples for the bending tests. For the research of optimal cutting speed only two states exists. If there is a crack the materials will be completely cut through in one step. The second state is where no crack is formed. From a variation of cutting speed a wide range of possible feed rates were found. The main focus for the investigations of the thermally induced cutting process was its ability to produce a certain edge quality. Therefore moderate parameters depicted in Figure 5 are chosen.

To compare the cutting technology with other dicing technologies, the material thickness of the wafer is s = 220 µm and is cut in one step.

4.2 Bending strength of crystalline silicon

If the fracture strength of crystal silicon is exceeded, the samples break. In dependence of the fracture strength, which mainly is influenced by the edge defects due to laser processing, the fracture behavior varies. In Figure 6, three exemplary broken samples are shown with their corresponding fracture load. It is obvious that a higher fracture load leads to higher internal stress. Here the sample will be cracked into an undefined number of parts while for low strength only two or three parts are normal.

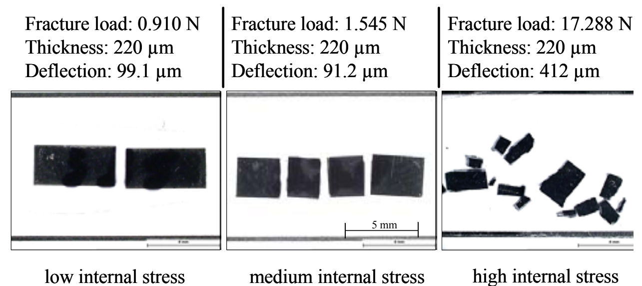

Fig. 6 Breakage in dependence of fracture load for 220 µm thick samples with <100> orientation.

The characteristic strengths are determined by the Weibull statistics explained in Chapter 3. In Figure 7, the strength is shown for the samples cut with the listed parameters from Table 3. To get a general overview, samples with the same dimensions are cut by a conventional sawing process with 20.000 revolutions per minute, a cutting velocity of $Vf = 2$ mm / s. The width of the sawing blade is $s = 45$ µm and grain of 4-6 µm.

The characteristic strength of the different laser cut samples are shown with a 90 % confidence interval. The second parameter extracted from the bending tests is the Weibull modulus m. The modulus is listed in Table 4 for the same parameters shown in Figure 7. The results show that there is not a significant difference between laser cut samples using ablation technologies except for picosecond laser pulses.

(Received: June 16, 2008, Accepted: October 1, 2008)

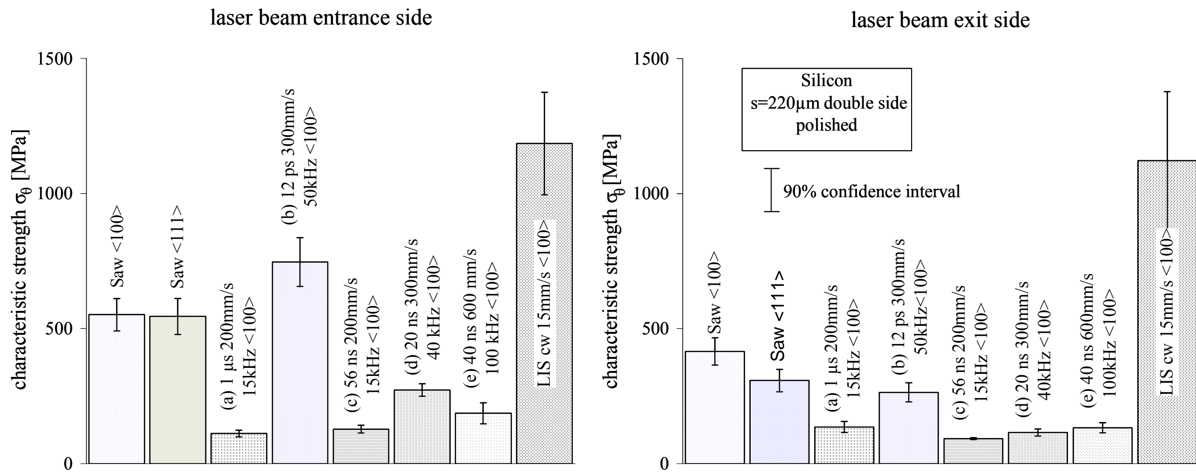

Fig. 7 Characteristic bending strength of silicon samples cut by mechanical saw and with different laser pulse durations.

Table 4 Characteristic strength σ_l and Weibull modulus m of laser and conventionally cut samples.

Laser	charct. Strength σ_σ [MPa]	90% confidence	Weibull modulus m	90% confidence	charact. Strength σ_0 [MPa]	90% confidence	Weibull modulus m	90% confidence
Saw <100>	551.18	± 59.79	5.54	± 0.64	415.96	± 50.95	6.24	± 0.55
Saw <111>	545.12	± 66.75	3.65	± 0.72	307.88	± 41.38	4.39	± 0.45
a StarDisc	111.91	± 12.33	4.66	± 0.13	135.76	± 20.45	3.98	± 0.22
b Staccato	746.44	± 23.18	8.96	± 0.13	264.33	± 11.91	7.18	± 0.13
c TLQ20	127.91	± 14.37	5.05	± 0.16	92.81	± 3.58	15.19	± 0.04
d Avia 7	272.82	± 23.35	6.75	± 0.25	115.66	± 12.90	6.93	± 0.14
e Avia 20	186.75	± 38.45	2.26	± 0.41	133.05	± 18.80	4.53	± 0.20
LIS SP200	1185.25	± 189.73	3.83	± 2.04	1121.65	± 256.15	2.83	± 2.76
	laser beam (saw) entrance side				laser beam (saw) exit side			

As shown in Table 4 the highest strength of the samples can be reached using thermally induced stress dicing. The high internal stress for the LIS leads to higher scattering which can be shown by comparing the Weibull-modulus. The scattering for the picosecond laser is low on the beam entrance and exit side which can be explained by the excellent quality of the cut edge.

5. Discussion

Laser dicing of crystalline silicon plays an important role if high accuracy and high cutting speed is necessary. In this paper, laser dicing technologies are compared by bending strength which directly correlates to the edge defects.

No significant differences can be observed for the ablation depths using different wavelengths. As predicted, the edge quality increases with decreasing pulse duration if the pulse duration decreases significantly as shown in Table 4. As shown, the bending strength of silicon samples is comparable for conventionally sawed and samples produced with picoseconds.

However, LIS combines both higher strength and higher effective cutting speed. The generated cutting edge have no defects which produces a higher bending strength with a factor of 4 compared to the conventional sawing technology and a factor of approx. 10 compared to laser dicing by ablation technology with pulse durations form micro- to nanoseconds.

Furthermore, it is shown that at the laser beam entrance side, higher strengths are measured. This can be explained by the multiple pass of the beam at the surface which leads to a smoothing or polishing effect and reduces the damages. At the exit side for all techniques, lower strengths are measured. Due to reflection and polarizing effects, the beam path deviated in the depth of the groove using a multiple path cutting technology. At the last passes before the sample is cut through, some parts of the silicon break and leads to edge defects, which can not be removed.

For thermally induced stress cutting, the differences between the laser beam entrance and exit side is much smaller than for the ablation technologies. Only a difference of approx. 5 % between both sides is measured while for the ablation techniques a variation from 21 % to 183 % occurs. The sample a) shows the inverse behavior. Here, the minimum number of passes is chosen so that some parts would only separate when picking up the parts.

A quantitative analysis of all different cut edges shows the range of reachable surface quality. In Table 5, the results are shown to give a measured area (A) of 694 X 233 µm^2 and a line measurement (L) in the middle of the cut edge with a length of 694.41 µm. The best quality over the whole area is reached by the saw followed by the AVIA7 laser with corresponding parameters. High values for the other ablation types are caused by the waviness of the edge due to the printing of the pulses and evaporated or melted material. In Figure 8 SEM pictures of laser diced edges for the different lasers and pulse durations are shown. The best visual edge quality corresponds to the characteristic strength of the dies.

Table 5 Average surface topography of cut silicon samples using different dicing technologies.

Laser/tool	Ra (A) [µm]	Rz (A) [µm]	Ra (L) [µm]	Rz (L) [µm]
Saw <100>	0.625	14.332	0.249	1.360
Saw <111>	0.812	14.946	0.327	1.432
a StarDisc	2.224	30.402	1.882	11.160
b Staccato	2.869	44.210	0.997	17.666
c TLQ20	3.858	27.207	3.870	19.049
d Avia7	1.362	14.230	0.686	10.659
e Avia20	0.838	21.728	0.686	12.218
LIS SPI200	0.324	27.624	0.248	1.130

(measured area 694.41 X 232.69 µm^2, line 694.41 µm, confocal microscope)

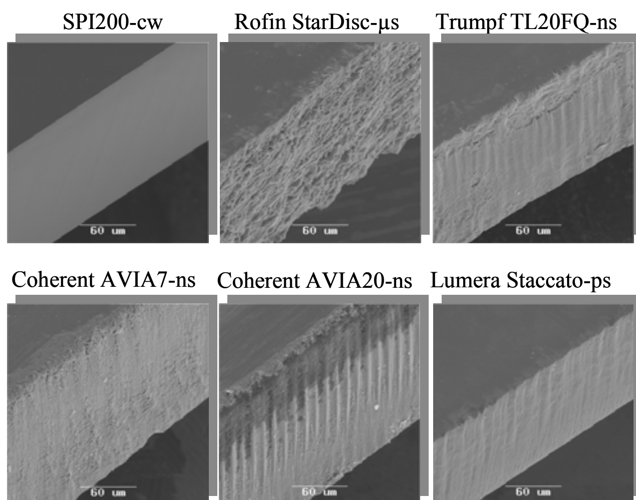

Fig. 8 SEM images of laser cut crystalline silicon samples with different mechanism, wavelengths and pulse durations.

6. Conclusion

This study shows the influence of pulse duration for the laser dicing of silicon. For the first time a complex study of different laser types with corresponding pulse durations, wavelengths and cutting mechanisms is done. The strength of the dies is compared by using the 3-point bending test.

The highest strength is achieved using the new LIS process in orders of 2 to 10 times compared to sawing and ablation processes. For Ultra-short pulse lasers the strength on the beam entrance side is comparable to a conventional sawing process. Micro- or nanosecond pulses lead to edge defects and reduce the strength of the samples and are below the strength of a conventional process. A trend for ablation mechanisms can be shown with decreasing pulse duration the strength increases. We can show the correlation between the far better edge quality and much higher edge strength of the new LIS process for the dicing of crystalline silicon.

References

[1] P. Chall: ALSI´s Low Power Multiple Beam Technology for High Throughput and Low Damage Wafer Dicing. In: Proceedings of 65th Laser Material Conference. (2006) p.211-215

[2] B. Richerzhagen, et al.: Dicing of wafers by patented water-jet-guided laser: the total damage free cut. In: Proceedings of 65th Laser Material Conference. (2006) p.197-200

[3] M. Kumagagi, et al.: Advanced Dicing Technology for Semiconductor Wafer – Stealth Dicing. In: J. IEEE Transactions on Semiconductor Manufacturing. Vol.20, No.3, (2007) p. 259-265

[4] L. Migliore, et al.: Advances in Laser Singulation of Silicon. In: Proceedings of International Congress on Applications of Lasers & Electro-Optics. (2006) p. 237-242

[5] A. Ostendorf, et al.: Flexible Laser Micro Machining of Semiconductors Materials using Frequency-Quadrupled Solid-State Lasers. In: Proceedings of Micro System Technology (2003) p. 248-255

[6] B. N. Chichkov, et al.: Femtosecond, picosecond and nanosecond laser ablation of solids. In: J. of Applied Physics, A 63 (1996) p. 109-115

[7] G.E. Jellison, et al.: Optical constants for silicon at 300 and 10 K determined from 1.64 to 4.73 eV by elipsometry. In: J. of Applied Physics, 53 (1982) 5

[8] D. Bäuerle: Laser Processing and Chemistry. 3. Edition. Heidelberg: Springer Verlag, 2000. –ISBN 3-540-66891-8

[9] M. v. Allmen, A. Blatter: Laser-Beam Interactions with Materials. 2. Edition. Heidelberg: Springer Verlag, 1998. - ISBN 3-540-59401-9

[10] A. Schoonderbeek, et al.: Laser Technology For Cost Reduction in Silicon Solar Cell Production. In: Proceedings of the 69th Laser Materials Processing Conference. (2007) p. 85-90

[11] A. Schoonderbeek, et al.: Laser technology for solar cells and solar receivers. In: Proceedings of International Congress on Applications of Lasers & Electro-Optics. (2007) p. 133-142

[12] B. Cotterell, Z. Chen, J.B. Haan, N.X. Tan: The strength of the silicon die in flip-chip assemblies. J. Electron Packaging (2003) 125, p.114-119

[13] S. Schoenfelder, et al.: Investigations of influence of dicing techniques on the strength properties of thin silicon. Microelectronics Reliability 47 (2007) p. 168-178

(Received: June 16, 2008, Accepted: October 1, 2008)